Front. Chem. Sci. Eng. 2023, 17(7): 867−879
https://doi.org/10.1007/s11705-022-2277-5

RESEARCH ARTICLE

Immobilization of laccase on organic–inorganic nanocomposites and its application in the removal of phenolic pollutants

Wei Zhang, Runtang Liu, Xu Yang, Binbin Nian, Yi Hu (✉)

State Key Laboratory of Materials-Oriented Chemical Engineering, School of Pharmaceutical Sciences, Nanjing Tech University, Nanjing 210009, China

Abstract Polydopamine-functionalized nanosilica was synthesized using an inexpensive and easily obtainable raw material, mild reaction conditions, and simple operation. Subsequently, a flexible spacer arm was introduced by using dialdehyde starch as a cross-linking agent to bind with laccase. A high loading amount (77.8 $mg \cdot g^{-1}$) and activity retention (75.5%) could be achieved under the optimum immobilization conditions. Thermodynamic parameters showed that the immobilized laccase had a lower thermal deactivation rate constant and longer half-life. The enhancement of thermodynamic parameters indicated that the immobilized laccase had better thermal stability than free laccase. The residual activity of immobilized laccase remained at about 50.0% after 30 days, which was 4.0 times that of free laccase. Immobilized laccase demonstrated excellent removal of phenolic pollutants (2,4-dichlorophenol, bisphenol A, phenol, and 4-chlorophenol) and perfect reusability with 70% removal efficiency retention for 2,4-dichlorophenol after seven cycles. These results suggested that immobilized laccase possessed great reusability, improved thermal stability, and excellent storage stability. Organic–inorganic nanomaterials have a good application prospect for laccase immobilization, and the immobilized laccase of this work may provide a practical application for the removal of phenolic pollutants.

Keywords polydopamine, pollutant removal, thermodynamic, phenolic pollutants, immobilized laccase

1 Introduction

Water pollution has become a rising concern with the accelerating growth of the global economy in recent years due to the large amount of industrial waste being discharged into water bodies without any systematic management. In particular, phenolic pollutants can pose a serious threat to humans, animals, and aquatic organisms even at very low concentrations due to their toxicity, carcinogenicity, mutagenicity, and poor biodegradability. Therefore, developing methods to treat phenolic wastewater is particularly important. The traditional treatment strategies for phenolic pollutants mainly include physical, chemical, and physicochemical methods. Although physicochemical methods have the advantage of high removal efficiency, the drawbacks such as energy consumption, high costs, and secondary pollution limit their further applications [1,2]. Recently, biological treatment technology has attracted increasing attention due to its high cost-effectiveness, wide range of applications, and high efficiency in the removal of phenols (PHs) [3]. It is considered an attractive and promising alternative method for the removal of a wide range of phenolic pollutants in water.

Laccase (E.C.1.10.3.2) is a series of multi-copper oxidases which utilizes molecular oxygen as an electron acceptor and is capable of catalyzing the simultaneous reduction of a wide range of phenolic compounds and aromatic amines to water with its co-substrate oxygen [4,5]. Laccase has been widely used in the fields of biofuel cells, biosensors, bioremediation, and wastewater treatment due to its excellent substrate specificity [6,7]. However, its low operational stability and difficulties in separation and reuse limit its practical use. How to effectively improve stability and reusability and maintain the activity of laccase has become a hot topic of research [8]. Immobilization technology is a fundamental means of achieving enzyme cost targets and realizing the advantages of enzyme technology. The immobilized enzyme can be easily separated from the product,

Received August 11, 2022; accepted October 27, 2022

E-mail: huyi@njtech.edu.cn

simplifying the post-treatment process and facilitating the recovery and reuse of the enzyme [9]. The thermal stability, organic solvent tolerance, and storage stability may be further enhanced after immobilization, which is conducive to improving its value in practical applications [10]. Currently, nanocarriers have been widely used in the field of immobilized enzymes because of their large specific surface areas, low mass transfer limits, easy recovery, and good stability [11,12]. Among nanomaterials, nanosilica (SiO_2) is widely used in nanoindustries, biotechnology, biomedical and pharmaceutical fields due to its low price, non-toxicity, large specific surface area, and additional advantages [13–15]. However, immobilizing enzymes directly on silica normally result in low catalytic performance due to the inherently inert surface properties of silica [16]. The surface modification of inorganic materials generally requires refluxing in organic solvents, which is not only time-consuming and laborious but also conducive to toxic solvents to remain in the pores of the material. This cumbersome process limits a wide range of practical applications [17]. Therefore, it is necessary to find a simple and environmentally friendly method to modify inorganic materials to prepare feasible carriers for the immobilization of enzymes. The dopamine molecule, containing catechol and an amino group, can form coatings on a variety of different substrates under weakly alkaline conditions, and these coatings can be easily functionalized and have a good application prospect [18]. The immobilization process is fast and easy with direct contact between the enzyme and the carrier. However, the enzyme usually loses its three-dimensional structure, and its activity could be decreased [19–21].

Some investigations have shown that the introduction of a spacer arm can effectively avoid the undesired contact between enzyme and carrier, which is beneficial to keeping the active conformation of the enzyme [22]. In particular, some water-soluble macromolecular polysaccharides such as dialdehyde polysaccharide [23], dialdehyde cellulose [24], and dialdehyde starch (DAS) have good biocompatibility and abundant functional groups and may serve as excellent flexible chains to connect carriers and enzymes [25–27]. Furthermore, these water-soluble biopolymers can prevent particle agglomeration through electrostatic repulsion between the particles, and the increased flexibility reduces steric hindrance. As a long-chain polymer, DAS has abundant functional groups that can provide a high number of active sites for enzyme immobilization. The spacer arm formed by the introduction of DAS can direct the enzyme molecules away from the particle surface and reduce the steric hindrance for better enzyme immobilization, thus improving the overall catalytic efficiency [28,29]. In this paper, polydopamine (PDA) was coated on SiO_2 material by self-polymerization of dopamine and the flexible natural organic polymer DAS was introduced at the outer PDA film for constructing the organic–inorganic nanocomposites. Laccase molecules were immobilized on the surface of the carrier by Schiff base reactions. This paper aimed to develop a novel enzyme immobilization strategy with organic–inorganic nanomaterials for improving the reusability and thermal stability of the immobilized enzymes and promoting their application in the field of organic wastewater treatment. In addition, this study can also provide a theoretical basis for the industrial application of laccase. For a clearer understanding of these processes, the synthesis of the carrier and the immobilized laccase as well as its application in the degradation of phenolic wastewater is shown in Scheme 1.

2 Experimental

2.1 Materials

Laccase from *Aspergillus oryzae* was provided by Sunson Industry Group Co., Ltd. (Ningxia, China). Dopamine hydrochloride and 2,2′-azino-bis(3-ethylbenzothiazoline-6-sulfonic acid) (ABTS) were purchased from Energy Chemical (Shanghai, China). 2,4-Dichlorophenol (2,4-DCP), bisphenol A (BPA), PH, and 4-chlorophenol (4-CP) were purchased from Sinopharm Chemical Reagent Co., Ltd. (China). SiO_2 was supplied by XFNANO (Shanghai, China), and DAS was purchased from Tai'an Jinshan Modified Starch Co. An Amethyst C18-H chromatography column was purchased from Sepax Technologies, Inc. (USA).

2.2 Characterizations

Scanning electron microscopy (SEM) and transmission electron microscopy (TEM) were performed on a Hitachi FE-SEM SU8200 instrument (Japan) and a Hitachi HT7700 instrument (Japan), respectively. High-performance liquid chromatography (HPLC) was conducted on an UltiMate 3000 instrument (Thermo Fisher Scientific, USA). Fourier transform infrared (FTIR) spectroscopy was performed on a Nicolet iS5 FTIR spectrometer (Thermo Fisher Scientific, USA) in the wavelength range of 400–4000 cm^{-1}. Thermogravimetric analysis (TGA) was performed on a TGA 550 instrument (TA Instruments, USA) at 50–800 °C under nitrogen atmosphere using a heating rate of 10 °C·min^{-1}. The specific surface area characteristics were analyzed through nitrogen adsorption–desorption at 77 K on an ASAP 2020 automated surface area and porosity analyzer (Micromeritics, USA). The specific surface areas were calculated using the Brunner–Emmett–Teller (BET) method. The average pore size diameter and pore volume were calculated using Barrett–Joyner–Halenda model.

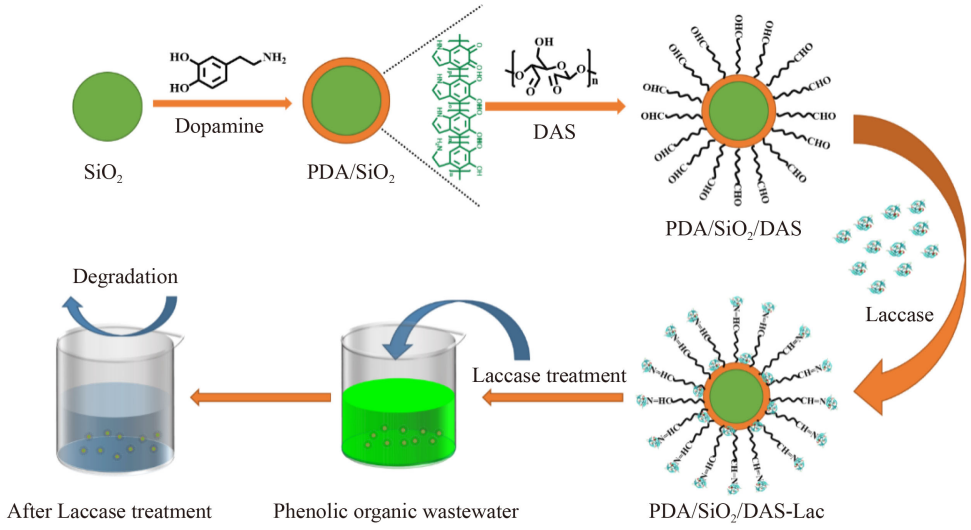

Scheme 1 Schematic illustration of the synthesis of PDA-functionalized nanoparticles, laccase immobilization, and application for pollutant removal.

2.3 Preparation of the PDA/SiO_2 and $DAS/PDA/SiO_2$ nanoparticles

The PDA/SiO_2 material was synthesized based on a previous report with some modifications [30]. Briefly, dopamine hydrochloride (100 mg) was dissolved in 100 mL of a Tris-HCl buffer solution (pH = 8.5) under magnetic stirring for 30 min. Then, 0.5 g SiO_2 was added to the solution. The suspension was vigorously stirred at room temperature for 12 h. Then, the solid was separated by centrifugation and washed several times with deionized water and ethanol to remove unreacted dopamine. Finally, the sample was obtained after vacuum drying and designated PDA/SiO_2.

To synthesize DAS-functionalized PDA/SiO_2, 100 mg PDA/SiO_2 was sonicated in 100 mL buffer solution (10 mmol·L^{-1}, pH = 7.0), followed by the addition of different amounts of DAS and magnetic stirring for 12 h at room temperature. The material was collected by centrifugation, washed several times with ethanol and deionized water, and dried under vacuum. The obtained composite material was designated $DAS/PDA/SiO_2$.

2.4 Laccase immobilization process

The $DAS/PDA/SiO_2$ carrier (10 mg) was dispersed in a buffer solution (citric acid and disodium hydrogen phosphate) under ultrasonic treatment. The laccase was dissolved in this dispersion to obtain a mixture of 0.6 mL laccase per mL dispersion, which was incubated at 30 °C for 4 h (pH = 3.5). The mixture was centrifuged and washed with the corresponding buffer solution until no protein was detected in the washing solution. The supernatant and wash solutions were collected, and the laccase loading was calculated using the Bradford method [31]. Finally, the immobilized laccase was obtained after freeze-drying and designated $DAS/PDA/SiO_2$-Lac. The immobilization process of condition optimization was consistent with the above except that the optimization conditions were different. Laccase was immobilized on SiO_2 and PDA/SiO_2 supports under the same conditions for comparison of the immobilization abilities of the different carriers.

2.5 Effect of conditions on immobilization

The effects of DAS dosage (0.5%–3.0%, m/v), laccase concentration (0.2–0.7 mL·mL^{-1}), immobilization time (1–10 h), temperature (25–50 °C), and pH (2.5–5.0) on the properties of $DAS/PDA/SiO_2$ were investigated. The relative activity and protein loading of immobilized laccase were studied. The initial conditions were an enzyme addition of 0.5 mL·mL^{-1}, a temperature of 25 °C, an immobilization time of 4 h, and pH 3.0. Each variable was measured three times in parallel, and the average value was taken as the experimental result. The relative activity, residual activity, and laccase loading were calculated according to the following equations:

$$\text{Relative activity}\,(\%) = \frac{A_i}{A_{max}} \times 100\%, \quad (1)$$

$$\text{Residual activity}\,(\%) = \frac{A_i}{A_{ini}} \times 100\%, \quad (2)$$

$$\text{Laccase loading}\,(\text{mg/g}) = \frac{C_0 \times V_0 - C_1 \times V_1}{M}, \quad (3)$$

where A_i is the absorbance, A_{max} is the maximum absorbance, and A_{ini} is the initial absorbance value of the samples, C_0 is the initial protein concentration of the laccase solution (mg·mL^{-1}), V_0 is the total volume of laccase added (mL), C_1 is the protein concentration of the wash solution (mg·mL^{-1}), V_1 is the total volume of the wash solution (mL), and M is the mass of the carrier (g).

2.6 Laccase activity assay

The laccase activity was evaluated by monitoring the oxidation of ABTS using the method described in previous literature [28]. An appropriate amount of free laccase and immobilized laccase were added to 5 mL ABTS buffer solution (0.1 mmol·L^{-1}) composed of citric acid and disodium hydrogen phosphate (0.15 mol·L^{-1}), reacted at 25–50 °C and pH of 2.5–5.0 for 5 min. The oxidation of ABTS was determined by spectrophotometry at a wavelength of 420 nm. Immobilization conditions were optimized for the determination of enzyme activity at 30 °C and pH 3.0.

2.7 Optimum temperature and pH for free laccase and immobilized laccase

The effects of pH and temperature on the activities of free and immobilized laccase were determined at various pH (2.5–5.5) and temperatures (25–55 °C). The effect of pH was determined in a buffer solution (pH 2.5–5.5) at 30 °C. The optimum temperature was determined under the respective optimum pH conditions. The maximum laccase activity was defined as 100% for free laccase and immobilized laccase.

2.8 Determination of kinetic parameters

The kinetic parameters of enzymes are important indicators for their evaluation. The kinetic properties of free laccase and immobilized enzyme were evaluated by the Michaelis–Menten kinetic model. The enzymatic activity was determined by adding equal amounts of enzymes in 5 mL of a buffer solution with different ABTS concentrations and reacting at the respective optimum pH and temperature for 5 min. The dynamic parameters were calculated through the Lineweaver–Burk diagram:

$$\frac{1}{V}=\frac{K_{\mathrm{m}}}{V_{\max}[\mathrm{S}]}+\frac{1}{V_{\max}}, \tag{4}$$

where [S] (mmol·L^{-1}) is the concentration of the substrate, V (μmol·L^{-1}·min^{-1}) is the reaction rate, K_{m} is Michaelis constant, and $V_{\max}$ is maximum reaction rate.

2.9 Storage stability of free laccase and immobilized laccase

Storage stability is an important indicator to evaluate the industrial application of laccase. Free laccase and immobilized laccase were stored at 4 °C for one month, and the laccase activity was measured every five days at the optimum temperature and pH. The activities prior to storage were defined as 100%.

2.10 Kinetic and thermodynamic parameters

The kinetic and thermodynamic parameters were calculated according to the description in previous literature with some modifications [32,33]. To study the thermal stability, free laccase and immobilized laccase were incubated at different temperatures in the range of 30–50 °C for up to 60 min. The residual activity of the samples was determined at different times under optimal reaction conditions, and the activity was defined as 100% for 0 min incubation time. The first-order thermal deactivation rate constant (k_{d}) was estimated by the linear regression between the logarithm of residual activity (%) and inactivation time (min). The half-life ($t_{1/2}$) was estimated by Eqs. (5) and (6):

$$Slope=k_{\mathrm{d}}, \tag{5}$$

$$t_{1/2}=\frac{\ln 2}{k_{\mathrm{d}}}. \tag{6}$$

The deactivation energy (E_{d}) of free and immobilized laccase was estimated from the Arrhenius plot (logarithm of the deactivation rate constant ($\ln k_{\mathrm{d}}$) versus the reciprocal of the temperature in Kelvin (1000/T)):

$$Slope=-\frac{E_{\mathrm{d}}}{\mathrm{R}}. \tag{7}$$

The change in enthalpy ($\Delta H°$, kJ·mol^{-1}), Gibbs free energy ($\Delta G°$, kJ·mol^{-1}), and entropy ($\Delta S°$, J·mol^{-1}·K^{-1}) for the thermal denaturation of free enzyme and immobilized enzyme were determined using the following equations:

$$\Delta H^{\circ}=E_{\mathrm{d}}-\mathrm{R}T, \tag{8}$$

$$\Delta G^{\circ}=-\mathrm{R}T\ln\frac{k_{\mathrm{d}}\times h}{k_{\mathrm{B}}\times T}, \tag{9}$$

$$\Delta S^{\circ}=-\frac{\Delta H^{\circ}-\Delta G^{\circ}}{T}, \tag{10}$$

where E_{d} is the activation energy for denaturation (kJ·mol^{-1}), T is the corresponding absolute temperature (K), R is the gas constant (8.314 J·mol^{-1}·K^{-1}), k_{d} is the deactivation rate constant (min^{-1}), k_{B} is the Boltzmann constant (1.38×10^{-23} J·K^{-1}), and h is the Planck constant (11.04×10^{-36} J·min).

2.11 Removal of organic pollutants

The catalytic performance of free and immobilized laccase was investigated by the removal of phenolic pollutants. Free and immobilized laccase were mixed with 2,4-DCP, BPA, PH, or 4-DCP (10 mg·L^{-1}) and reacted at optimal pH and room temperature. The supernatant was analyzed by HPLC under the following test conditions: the mobile phase for 2,4-DCP and BPA pollutants was 70% aqueous methanol solution. The mobile phase system of PH and 4-DCP pollutants was a mixture of 0.1% aqueous formic acid solution and methanol (35:65, v/v); the column temperature and flow rates were 30 °C and 1.0 mL·min^{-1}, respectively, and the

detection time was 10 min. The detection wavelength of BPA was 290 nm, and the other phenolic pollutants were detected at 220 nm. The removal efficiency was calculated by the following equation:

$$\text{Removal efficiency}\,(\%) = \frac{C_0 - C_i}{C_0} \times 100\%, \qquad (11)$$

where C_0 (mg·L^{-1}) is the initial concentration of phenolic pollutant, and C_i (mg·L^{-1}) is the concentration of phenolic pollutant after laccase treatment at time.

3 Results and discussion

3.1 Determination of preparation conditions for DAS/PDA/SiO_2-Lac

The results of the optimization of the immobilization conditions of laccase are shown in Figs. S(1)–S(5) (cf. Electronic Supplementary Material), indicating the following optimal conditions: DAS and laccase concentrations of 1.5% (*m*/*v*) and 0.6 mL·mL^{-1}, respectively; an immobilization time of 4 h, a temperature of 30 °C, and pH 3.5. To compare the loading capacity and activity retention of the SiO_2, PDA/SiO_2, and DAS/PDA/SiO_2 carriers, a summary is provided in Table 1. The loading capacity of DAS/PDA/SiO_2 was up to 77.8 mg·g^{-1} under the optimum conditions, which was 1.1 and 4.0 times higher than that of the SiO_2 and PDA/SiO_2 supports, respectively. The activity retention of DAS/PDA/SiO_2-Lac (75.5%) was higher than that of PDA/SiO_2-Lac (66.3%) and SiO_2-Lac (32.5%). The main reason for this difference was that the introduction of DAS increased the number of aldehyde groups, which allowed the carrier to better covalently combine with the laccase through chemical reactions (Michael addition and Schiff base reaction). The activity retention was significantly higher than that of laccase immobilized on amino-functionalized SiO_2 (25.6%) and on ionic-liquid-modified SiO_2 (66.0%) reported in the literature [34]. The introduction of natural organic polymers was beneficial to maintaining the secondary and tertiary structure of the laccase, preserving the conformation of laccase, reducing the loss of laccase during immobilization, and improving its activity retention rate [35].

Table 1 Result of immobilization of laccase

Support	Added laccase /(mL·mL^{-1})	Laccase loading /(mg·g^{-1})	Activity retention/%
SiO_2	0.6	19.2	32.5
PDA/SiO_2	0.6	68.3	66.3
DAS/PDA/SiO_2	0.6	77.8	75.5

3.2 Results of FTIR spectroscopy and TGA of materials

The FTIR spectra and TGA cueves are shown in Fig. 1. The FTIR spectra of DAS, SiO_2, PDA/SiO_2, and DAS/PDA/SiO_2 are shown in Fig. 1(a). Typical peaks of DAS were observed at 2921 and 1725 cm^{-1}, attributed to the stretching vibration of C–H and C=O of the aldehyde group, respectively [28]. The spectrum of SiO_2 had strong absorption peaks at 1079, 965, and 803 cm^{-1}. The peak at 1079 cm^{-1} belonged to the asymmetric stretching vibration of the Si–O–Si bond, and the absorption peaks at 965 and 803 cm^{-1} corresponded to the symmetrical stretching vibration of Si–O groups [35]. The characteristic peaks of SiO_2 were retained with the introduction of PDA. At the same time, a new absorption peak was observed at 1517 cm^{-1}, which was assigned to C–C bond vibrations of the aromatic rings of PDA [36]. The results demonstrated that PDA/SiO_2 was successfully synthesized. After the modification of PDA/SiO_2 with DAS, the peak at 1079 cm^{-1} was broadened, which might be caused by the presence of C=N vibrations as a result of the Schiff base reaction between DAS and PDA. In addition, the characteristic absorption peak of DAS could also be found at 2921 cm^{-1}. The results showed that the DAS/PDA/SiO_2 carrier was successfully prepared.

Using TGA (Fig. 1(b)), the amount of PDA and DAS

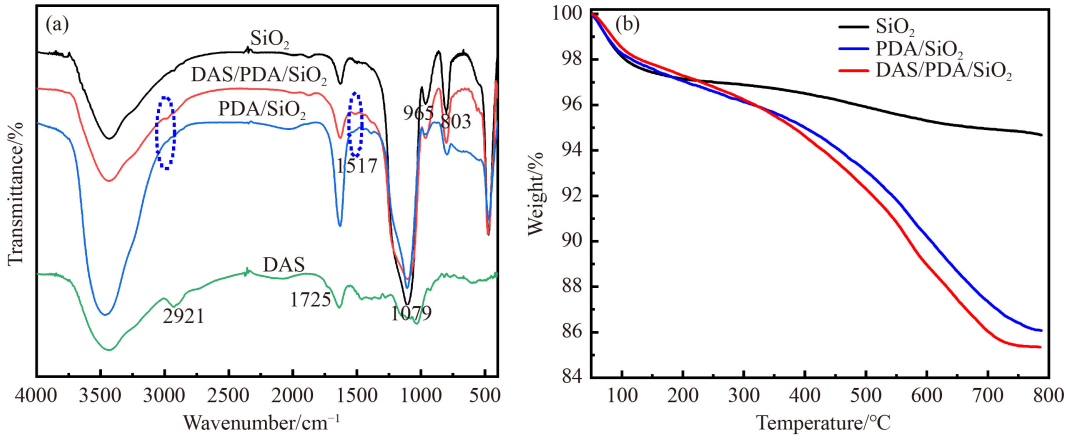

Fig. 1 (a) FTIR spectra and (b) TGA curves of carriers.

on the surface of SiO_2 particles was quantified by calculating the weight loss at different temperature stages. The weight loss of SiO_2 was about 5% during the entire process, while the total weight losses of PDA/SiO_2 and DAS/PDA/SiO_2 were 14% and 15%, respectively. The samples had similar weight losses below 100 °C, which was mainly due to the loss of free water and solvent on the sample surfaces. PDA/SiO_2 and DAS/PDA/SiO_2 had similar weight loss curves, and the weight loss of the samples increased rapidly above 100 °C, which was related to the decomposition of PDA coated on the SiO_2 surface. Finally, the total weight loss of DAS/PDA/SiO_2 was about 1% higher than that of PDA/SiO_2, which was attributed to the decomposition of DAS on the PDA/SiO_2 surface. The TGA results confirmed the successful synthesis of the DAS/PDA/SiO_2 support. This conclusion was consistent with the results of FTIR spectroscopy.

3.3 SEM of free laccase and immobilized laccase

The SEM and TEM images of SiO_2 and DAS/PDA/SiO_2 are shown in Fig. 2. The morphology of SiO_2 shown in Fig. 2(a) was still well preserved after modification by PDA and DAS (Fig. 2(d)), indicating that SiO_2 could maintain excellent stability during immobilization. This conclusion was consistent with the results of FTIR spectroscopy. According to the TEM characterization, SiO_2 nanoparticles were spherical with a diameter of about 20 nm and slightly aggregated. After PDA and DAS modification, the exposed SiO_2 nanoparticles were coated with another layer (Fig 2(f)), and the particles exhibited better dispersion, which can be attributed to a weaker interaction between the particles caused by the coating on the surface of SiO_2. The above results proved that the modification of SiO_2 nanoparticles was successful. The material possessed the advantages of the inorganic carrier and provided a useful basis for improving the stability of immobilized enzymes in the later stages.

3.4 BET analysis of materials

The nitrogen adsorption–desorption isotherms for SiO_2, PDA/SiO_2, and DAS/PDA/SiO_2 are shown in Fig. 3, and the pore structure properties of the supports are listed in Table 2. The BET specific surface area of SiO_2 decreased with the introduction of PDA and then increased with the introduction of DAS. As possible reasons, the pores were partially filled with PDA nanoparticles after the introduction of PDA, which affected the specific surface area of the carrier; then, the surface area of DAS/PDA/SiO_2 was increased because of the presence of DAS on the PDA/SiO_2 sample surface after being anchored through Schiff base reactions. Laccase has sufficient space to expand its three-dimensional structure with the increase in specific surface area, so that the laccase can better maintain its conformation, resulting in better activity on the carrier [37]. The average pore diameter and average total volume increased with the introduction of PDA and DAS, which might be due to the aggregation of PDA and DAS on the SiO_2 surface or around existing pores to form new pores. The results were consistent with other results and again confirmed the successful fabrication of the support material.

3.5 Enzymatic activity of free laccase and laccase immobilized on DAS/PDA/SiO_2 nanoparticles

3.5.1 Effects of pH and temperature on free laccase and immobilized laccase

The catalytic activity of laccase is sensitive to pH and temperature, which limits its application in many fields. The appropriate temperature and pH are more conducive to maintaining the structural properties of laccase for maximal activity. To identify the optimal pH and temperature of free and immobilized laccase, the relative enzymatic activity was examined in the pH and temperature ranges of 2.5–5.5 and 25–60 °C, respectively. The results are shown in Fig. 4.

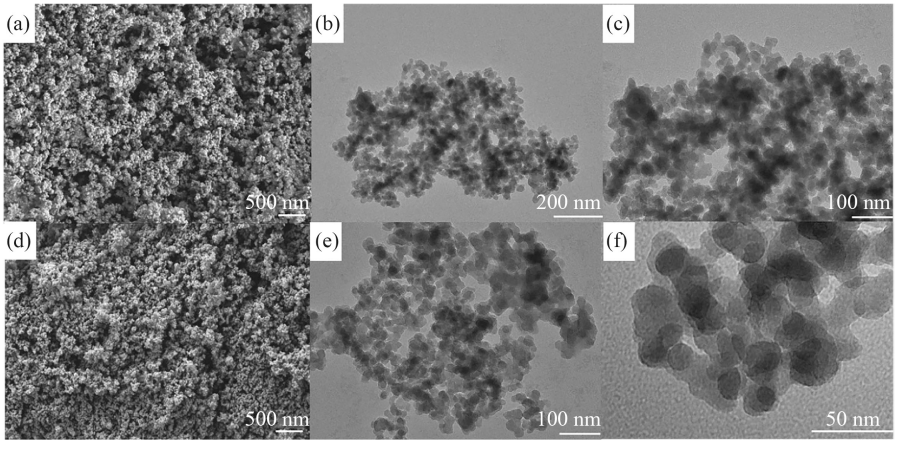

Fig. 2 SEM and TEM images of (a–c) SiO_2 and (d–f) DAS/PDA/SiO_2.

According to Fig. 4(a), the immobilized laccase had a wider acid tolerance range compared with free laccase. Laccase immobilized on the DAS/PDA/SiO_2 nanoparticles kept about 95% of its activity at pH 2.5, which was significantly higher than that of free laccase. In addition, the pH sensitivity of immobilized laccase was lower than that of free laccase in the pH range of 3.5–5.5. This may be due to the occurrence of ionization of acidic or basic amino side chains in the microenvironment surrounding the immobilized carrier amino groups, which enhances hydrogen bonding or electrostatic interactions between laccase and the carrier [38,39]. Furthermore, the introduction of the biopolymer DAS provided multiple attachment sites for laccase, allowing the enzyme molecule to be immobilized on the support material by multipoint attachment and resulting in a more stable conformation [37]. The covalent bonds, hydrogen bonds, or electrostatic interactions between the enzyme and the carrier during the cross-linking process result in higher stability of the immobilized enzyme.

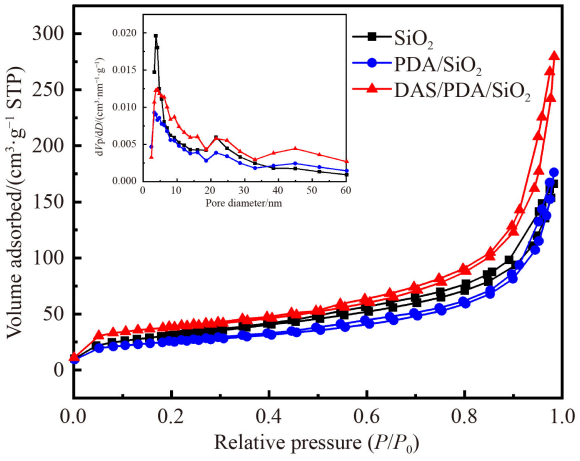

Fig. 3 Nitrogen sorption isotherms of SiO_2, PDA/SiO_2, and DAS/PDA/SiO_2.

Table 2 Pore structure properties of supports

Support	Specific surface area/($cm^2 \cdot g^{-1}$)	Average pore diameter/nm	Total pore volume/($cm^3 \cdot g^{-1}$)
SiO_2	111.13	9.24	0.26
PDA/SiO_2	89.82	12.15	0.27
DAS/PDA/SiO_2	135.48	12.77	0.43

Temperature is an important factor in the evaluation of the enzymatic properties of laccase. Too high temperatures will inactivate the enzyme and reduce the stability and half-life of the enzyme. The effect of temperature was evaluated in the range of 25–60 °C, and the results are shown in Fig. 4(b). The optimal temperature of free laccase was 30 °C, while the optimal temperature for immobilized laccase increased from 30 to 45 °C, and immobilized laccase was significantly less sensitive to temperature than free laccase. When the temperature reached 65 °C, the immobilized laccase could still maintain more than 40% activity, while the free laccase lost almost all activity. The main reason was that free laccase could easily denature at high temperatures, resulting in irreversible changes in secondary and tertiary structures [40,41]. The introduction of flexible long chains on the surface of nanoparticles could effectively improve the stability of laccase at high temperatures. In general, the immobilized laccase exhibited excellent resistance to low pH and high temperatures, which provided a feasible range of conditions for future industrial applications.

3.5.2 Kinetic parameters of enzymatic reactions

The kinetic parameters Michaelis constant K_m and maximum reaction rate V_{max} of free laccase and immobilized laccase were studied with different concentrations of ABTS as substrate, and the results are provided in Fig. 5 and Table 3. The affinity of immobilized laccase for the substrate (K_m = 0.870) did not change significantly compared to free laccase (K_m = 0.851), indicating that the

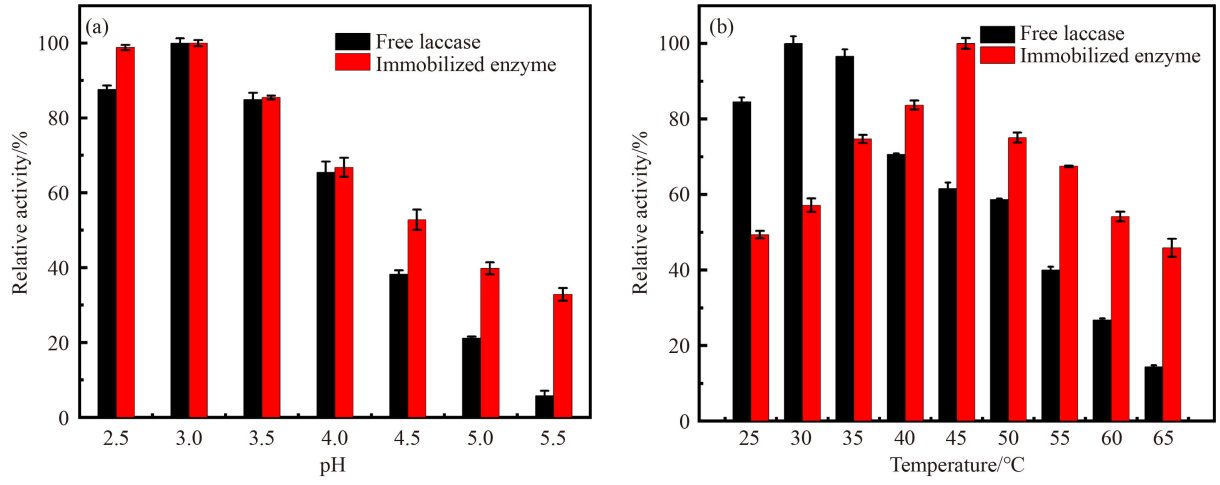

Fig. 4 Effect of (a) pH and (b) temperature on the relative activity of free and immobilized laccase.

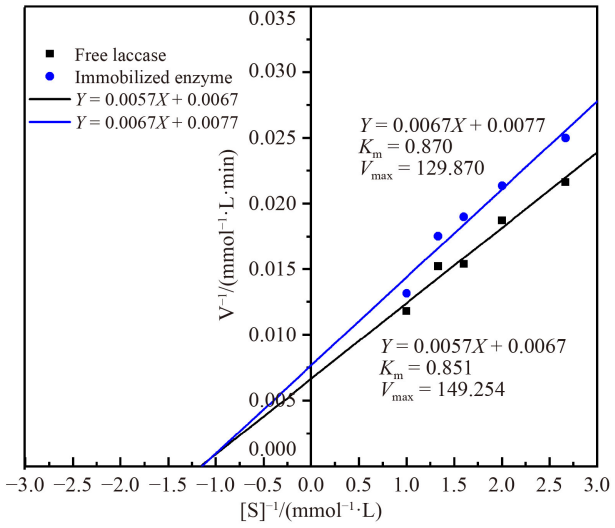

Fig. 5 Lineweaver–Burk plots of free and immobilized laccase.

Table 3 Kinetic parameters of immobilized laccase

Sample	K_m/(mmol·L^{-1})	V_{max}/(mmol·L^{-1}·min^{-1})	V_{max}·K_m^{-1}/min^{-1}
Free laccase	0.851	149.254	175.387
Immobilized laccase	0.870	129.870	149.276

affinity for the substrate remained after the immobilization of laccase. V_{max} was lower for immobilized laccase (V_{max} = 129.870) than for free laccase (V_{max} = 149.254). The decrease in V_{max} may be due to a steric hindrance effect of the carrier material on the catalytic site of laccase [26,42]. The substrate affinity was not reduced after immobilization, and the effective combination of enzyme and substrate provided a good foundation for the removal of water pollutants.

3.5.3 Kinetic and thermodynamic parameters

Thermal deactivation rate, deactivation half-life, and thermal deactivation energy are parameters that reflect the dynamics of the thermal deactivation of laccase. The kinetic parameters play a role in the catalysis by laccase because it provides information about the influence of temperature increase on laccase denaturation [43]. The thermal deactivation curves are shown in Fig. 6 and the results of kinetic parameters of thermal deactivation of free and immobilized laccase are summarized in Table 4. The k_d values of immobilized laccase and free laccase gradually increased with the increase in temperature, indicating that the stability of laccase gradually decreased. The k_d value of immobilized laccase was

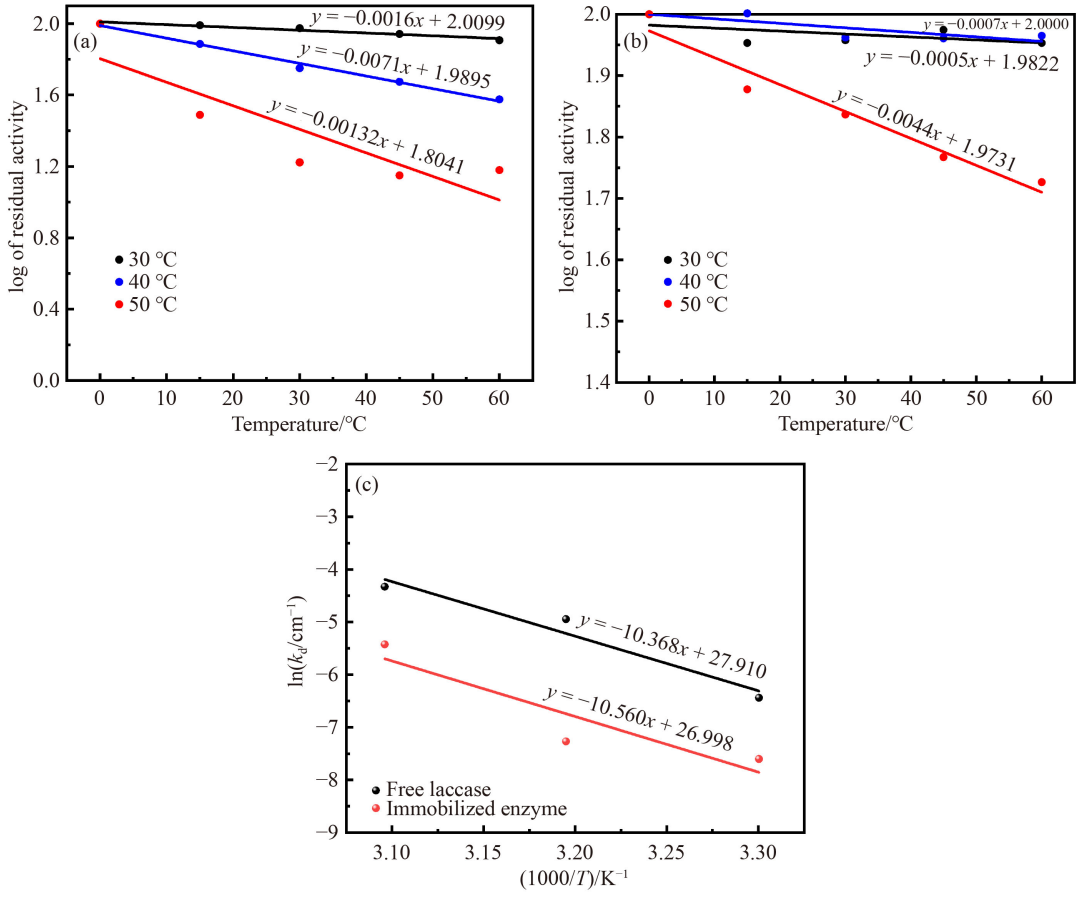

Fig. 6 Dynamic curves of thermal deactivation of (a) free laccase and (b) immobilized laccase; (c) Arrhenius plots for the thermal deactivation of free laccase and immobilized laccase.

smaller than that of free laccase at the same temperature, demonstrating that immobilized laccase had better stability than free laccase. As commonly known, a longer half-life indicates a better temperature tolerance of a sample [44]. The half-life of immobilized laccase was longer than that of free laccase in the temperature range of 30–50 °C. The reduction in the half-life of free laccase was mainly due to the destruction of the laccase structure, which was consistent with previous research results [32,36]. E_d of immobilized laccase was higher than that of free laccase, indicating that the laccase stability improved after the immobilization process [43]. The results showed that immobilized laccase had better stability and temperature tolerance than free laccase.

The thermodynamic parameters of free laccase and immobilized laccase are summarized in Table 5. The value of ΔH for free laccase at 30, 40, and 50 °C were 83.68, 83.59, and 83.51 kJ·mol^{-1}, respectively, and for immobilized laccase 85.28, 85.19, and 85.11 kJ·mol^{-1}, respectively. Immobilized laccase had a higher ΔH value than free laccase at the same temperature, indicating that more energy was required to denature immobilized laccase. The large ΔH values corresponded to high thermal stability, meaning that the laccase after immobilization had better temperature tolerance than the free laccase. The ΔG values decreased with increasing temperature and were higher for immobilized laccase than for free laccase at each temperature. The results meant that immobilized laccase had better stability and temperature tolerance than free laccase. A negative value for ΔS commonly indicates that entropy decreases as the transition state occurs, indicating that laccase oxidation of ABTS occurs autonomously without recourse to other means [45]. The results demonstrated that the stability of laccase was significantly improved after immobilization, which was consistent with the results of most immobilized laccase.

3.6 Degradation of phenolic pollutants by free and immobilized laccase

The catalytic activity of immobilized laccase was evaluated using common industrial phenolic pollutants as degradation model substrates. The results are shown in Fig. 7. A high removal rate was observed during the initial 6 h. In the next reaction stage, the removal rate gradually decreased, which might be related to the simultaneous decrease in the concentration of phenolic pollutants. After 6 h, the pollutants were hardly removed by free laccase, which might be due to the combination of the produced polymer with the active site of laccase molecules, preventing the substrate from binding to those sites and resulting in the destruction of the protein structure of laccase [46]. Compared with free laccase, the immobilized laccase still maintained high activity after 6 h, mainly because the introduction of DAS increased the flexibility of the immobilized laccase. Furthermore, the abundant functional groups on the surface of the support created multipoint links between the laccase molecules and the carrier, prevented the denaturation of protein molecules, and effectively improved the activity of immobilized laccase [20]. After 12 h, the 2,4-DCP removal rate by DAS/PDA/SiO_2-Lac was 100%, and the PBA removal rate was 88.2%, which was significantly higher than that of free laccase of 78.7% and 63.5%. This degradation efficiency was higher than the reported 87.0% 2,4-DCP removal by laccase immobilized on amino-functionalized magnetic metal–organic frameworks and 94.6% 2,4-DCP removal by laccase immobilized on halloysite nanotubes [47,48]. The BPA removal efficiency was significantly higher than that reported in literature [37,16]. The immobilized laccase could remove 85.1% PH and 84.2% 4-CP after 12 h, and the removal efficiencies were 2.0 times and 1.7 times those of free laccase, respectively. The removal efficiency was higher than obtained with laccase immobilized on epoxy-functionalized silica, which achieved 60.0% removal of PH and 76.0% removal of 4-CP [49]. DAS/PDA/SiO_2-Lac exhibited an obvious advantage in the removal of typical phenolic pollutants over similar catalysts reported in literature and proved wide application prospects in the removal of phenolic pollutants. The removal of phenolic pollutants by laccase immobilized on different carrier materials is summarized

Table 4 Kinetic parameters of thermal deactivation of free and immobilized laccase

Temperature/°C	K_d/min^{-1}			$t_{1/2}$/s			E_d/(kJ·mol^{-1})
	30	40	50	30	40	50	
Free laccase	0.0016	0.0071	0.0132	433.22	97.63	52.51	86.20
Immobilized laccase	0.0005	0.0007	0.0044	1386.29	990.20	157.53	87.80

Table 5 Thermodynamic parameters for thermal deactivation of free and immobilized laccase

Temperature/°C	ΔH/(kJ·mol^{-1})			ΔG/(kJ·mol^{-1})			ΔS/(J·mol^{-1}·K^{-1})		
	30	40	50	30	40	50	30	40	50
Free laccase	83.68	83.59	83.51	102.23	98.26	94.63	–61.22	–44.59	–39.25
Immobilized laccase	85.28	85.19	85.11	103.71	102.94	98.39	–60.84	–56.71	–41.12

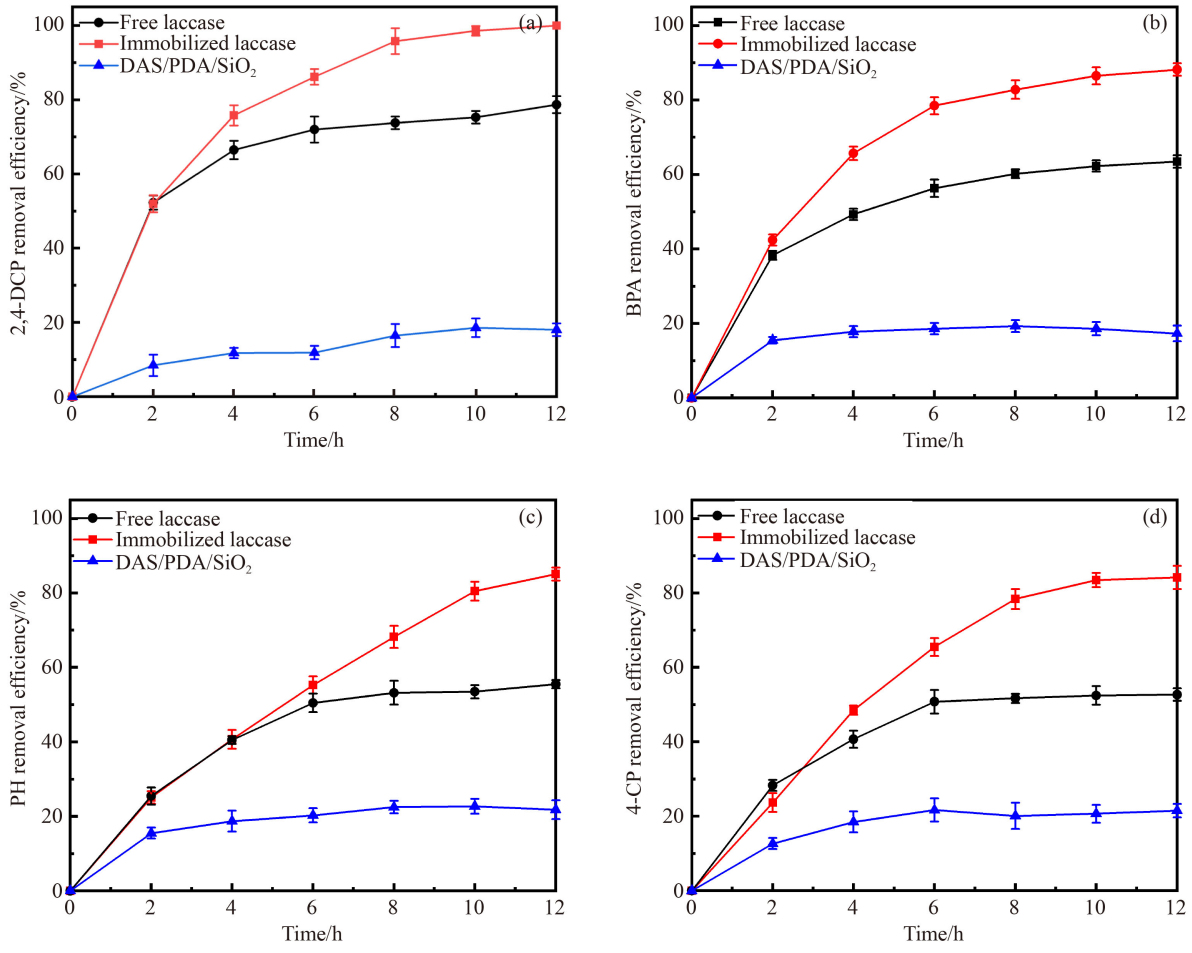

Fig. 7 Degradation curves of (a) 2,4-DCP, (b) BPA, (c) PH, and (d) 4-CP.

Table 6 Removals of phenolic compounds by different immobilized laccase catalysts

Support	Pollutants	Concentration/(mg·L^{-1})	Reaction time/h	Removal efficiency/%	Ref.
Amino-functionalized magnetic metal–organic framework	2,4-DCP	10	12	87.0	[47]
Halloysite nanotubes	2,4-DCP	10	24	94.6	[48]
Multi-walled carbon nanotubes	BPA	10	24	80.0	[50]
Amino-functionalized ionic liquid	4-CP	10	24	89.3	[28]
	2,4-DCP	10		100.0	
	PH	10		83.4	
PDA functionalized nano-silica	2,4-DCP	10	12	100.0	This work
	BPA	10		88.2	
	PH	10		85.1	
	4-CP	10		84.2	

in Table 6. A comparison of those results reveals that the immobilized laccase synthesized in this paper has a high removal efficiency of phenolic compounds and a broad application range in wastewater treatment.

3.7 Reusability and storage stability of immobilized laccase

Recycling ability and storage stability are essential requirements for industrial production. The immobilization of laccase is beneficial to the separation of product and laccase and the reuse of the catalyst. The results of reusability and storage are show in Fig. 8. The 2,4-DCP removal efficiencies for several cycles of used catalysts are shown in Fig. 8(a). In the seventh cycle, the immobilized laccase could still maintain a degradation efficiency of more than 70%. DAS/PDA/SiO_2-Lac exhibited better reusability compared with similar methods reported in literature [51–53]. The strong covalent binding of aldehyde groups to catechol on the surface of the carrier and to amine groups reduces the leaching of laccase from the carrier. At the same time, the existence

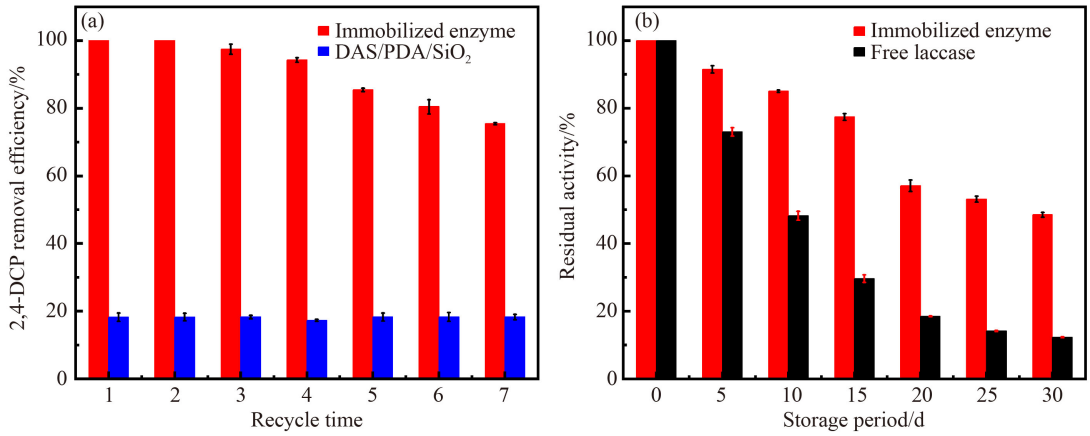

Fig. 8 (a) 2,4-DCP removal efficiencies of recycled immobilized laccase and (b) the residual activity of free laccase and immobilized laccase after storage.

of the flexible chain of the natural organic polymer DAS effectively reduced the occurrence of mechanical collisions between the support and laccase, so that the three-dimensional structure of the immobilized laccase was preserved. The decrease in activity might be due to adhesion of the polymer to the carrier surface during degradation or leaching of laccase molecules during use [28,37]. Organic and inorganic nanocomposites had the characteristics of organic, inorganic, and nanomaterials and great mechanical strength, stability, and biocompatibility. They could effectively enhance the enzymatic properties of immobilized laccase and had great application potential.

Storage stability is an important parameter in practical applications. The results of residual activity of catalysts stored for certain periods are shown in Fig. 8(b). The immobilized laccase retained more than 50% of the initial activity after 30 days, which was much higher than the activity retention of 10% of free laccase. The results showed that the organic–inorganic nanocomposites had a protective effect on laccase. As a possible reason, the covalent immobilization process may increase the structural rigidity of laccase and reduce the expansion of the protein, which played an important role in protecting laccase from potential environmental damage [54].

4 Conclusions

In this study, organic–inorganic nanocomposites (DAS/PDA/SiO_2) were successfully prepared by self-polymerization and cross-linking. The mechanical strength and stability of immobilized laccase were improved by using SiO_2 as inorganic carrier. The introduction of PDA effectively improved biocompatibility and reactivecoatings.Thefurtherintroductionofafunctionalbiological macromolecule, DAS, directed laccase away from the carrier surface, effectively improving loading capacity (77.8 $mg \cdot g^{-1}$) and activity retention (75.5%). After immobilization, the stability and catalytic activity were significantly improved. Immobilized laccase had a strong ability to treat phenolic pollutants and maintained an activity of more than 70% in the removal of 2,4-DCP after seven times of reuse. The organic–inorganic nanocomposites synthesized in this paper have the characteristics of both organic and inorganic materials and possess good mechanical strength, stability, and biocompatibility. These properties provide the possibility of screening laccase formulations and provide important theoretical studies to promote the application of new immobilized laccase catalysts in the field of wastewater treatment.

Acknowledgements This work was supported by the National Natural Science Foundation of China (Grant No. 22178174), the National Key R&D Program of China (Grant No.2021YFC2103802), and the Jiangsu Synergetic Innovation Center for Advanced Bio-Manufacture (Grant No. XTC2206).

Electronic Supplementary Material Supplementary material is available in the online version of this article at https://dx.doi.org/10.1007/s11705-022-2277-5 and is accessible for authorized users.

References

1. Zhou W, Zhang W, Cai Y. Laccase immobilization for water purification: a comprehensive review. Chemical Engineering Journal, 2020, 403: 126272
2. Arora P K, Bae H. Bacterial degradation of chlorophenols and their derivatives. Microbial Cell Factories, 2014, 13(1): 1–17
3. Rostami A, Abdelrasoul A, Shokri Z, Shirvandi Z. Applications and mechanisms of free and immobilized laccase in detoxification of phenolic compounds—a review. Korean Journal of Chemical Engineering, 2022, 39(4): 821–832
4. Fan J X, Luo J Q, Wan Y H. Aquatic micro-pollutants removal with a biocatalytic membrane prepared by metal chelating affinity membrane chromatography. Chemical Engineering Journal, 2017, 327: 1011–1020
5. Liu Y Y, Zeng Z T, Zeng G M, Tang L, Pang Y, Li Z, Liu C, Lei X X, Wu M S, Ren P Y, Liu Z, Chen M, Xie G. Immobilization

of laccase on magnetic bimodal mesoporous carbon and the application in the removal of phenolic compounds. Bioresource Technology, 2012, 115: 21–26

6. Fan J X, Luo J Q, Wan Y H. Membrane chromatography for fast enzyme purification, immobilization and catalysis: a renewable biocatalytic membrane. Journal of Membrane Science, 2017, 538: 68–76
7. Bilal M, Ashraf S S, Cui J D, Lou W Y, Franco M, Mulla S I, Iqbal H M N. Harnessing the biocatalytic attributes and applied perspectives of nanoengineered laccases—a review. International Journal of Biological Macromolecules, 2021, 166: 352–373
8. Qiu X, Qin J, Xu M, Kang L F, Hu Y. Organic–inorganic nanocomposites fabricated via functional ionic liquid as the bridging agent for laccase immobilization and its application in 2,4-dichlorophenol removal. Colloids and Surfaces B: Biointerfaces, 2019, 179: 260–269
9. Sheldon R A, van Pelt S. Enzyme immobilisation in biocatalysis: why, what and how. Chemical Society Reviews, 2013, 42(15): 6223–6235
10. Dicosimo R, Mcauliffe J, Poulose A J, Bohlmann G. Industrial use of immobilized enzymes. Chemical Society Reviews, 2013, 42(15): 6437–6474
11. Zhao J X, Ma M M, Yan X H, Zhang G H, Xia J H, Zeng Z L, Yu P, Deng Q, Gong D M. Green synthesis of polydopamine functionalized magnetic mesoporous biochar for lipase immobilization and its application in interesterification for novel structured lipids production. Food Chemistry, 2022, 379: 132148
12. Zhong L, Feng Y X, Wang G Y, Wang Z Y, Bilal M, Lv H X, Jia S R, Cui J D. Production and use of immobilized lipases in/on nanomaterials: a review from the waste to biodiesel production. International Journal of Biological Macromolecules, 2020, 152: 207–222
13. Jeelani P G, Mulay P, Venkat R, Ramalingam C. Multifaceted application of silica nanoparticles: a review. Silicon, 2020, 12(6): 1337–1354
14. Silvestri B, Vitiello G, Luciani G, Calcagno V, Costantini A, Gallo M, Parisi S, Paladino S, Iacomino M, D'Errico G, Caso M F, Pezzella A, d'Ischia M. Probing the eumelanin-silica interface in chemically engineered bulk hybrid nanoparticles for targeted subcellular antioxidant protection. ACS Applied Materials & Interfaces, 2017, 9(43): 37615–37622
15. Ni Y, Lv Z X, Wang Z, Kang S Y, He D W, Liu R J. Immobilization and evaluation of penicillin G acylase on hydroxy and aldehyde functionalized magnetic α-Fe_2O_3/Fe_3O_4 heterostructure nanosheets. Frontiers in Bioengineering and Biotechnology, 2022, 9(1): 812403
16. Lin J, Liu Y, Shi C, Le X, Zhou X, Zhao Z, Ou Y, Yang J. Reversible immobilization of laccase onto metal-ion-chelated magnetic microspheres for bisphenol A removal. International Journal of Biological Macromolecules, 2016, 84: 189–199
17. Chen Y, Ding H, Wang B, Shi Q, Gao J, Cui Z, Wan Y. Dopamine functionalization for improving crystallization behaviour of polyethylene glycol in shape-stable phase change material with silica fume as the matrix. Journal of Cleaner Production, 2019, 208: 951–959
18. Wang L, Shi Y, Chen S, Wang W, Tian M, Ning N, Zhang L. Highly efficient mussel-like inspired modification of aramid fibers by UV-accelerated catechol/polyamine deposition followed chemical grafting for high-performance polymer composites. Chemical Engineering Journal, 2017, 314: 583–593
19. Deng M, Zhao H, Zhang S, Tian C, Zhang D, Du P, Liu C, Cao H, Li H. High catalytic activity of immobilized laccase on core-shell magnetic nanoparticles by dopamine self-polymerization. Journal of Molecular Catalysis B: Enzymatic, 2015, 112: 15–24
20. Chen H, Hao Z, Li Y, Li Y, Wang X. Facile synthesis of oxidic PEG-modified magnetic polydopamine nanospheres for candida rugosa lipase immobilization. Applied Microbiology and Biotechnology, 2015, 99(3): 1249–1259
21. Chen Y, Jiang Y, Gao J, Wu W, Dong L, Yang Z. Facile immobilization of nitrile hydratase in SBA-15 via a biomimetic coating. Journal of Porous Materials, 2017, 24(3): 787–793
22. Zhang H R, Luo J Q, Li S S, Wei Y P, Wan Y H. Biocatalytic membrane based on polydopamine coating: a platform for studying immobilization mechanisms. Langmuir, 2018, 34(8): 2585–2594
23. Khan M K, Luo J Q, Wang Z S, Khan R, Chen X R, Wan Y H. Alginate dialdehyde meets nylon membrane: a versatile platform for facile and green fabrication of membrane adsorbers. Journal of Materials Chemistry B: Materials for Biology and Medicine, 2018, 6(11): 1640–1649
24. Wang S S, Li S, Liu R T, Zhang W, Xu H J, Hu Y. Immobilization of interfacial activated candida rugosa lipase onto magnetic chitosan using dialdehyde cellulose as cross-linking agent. Frontiers in Bioengineering and Biotechnology, 2022, 10: 946117
25. Ran F, Zou Y, Xu Y, Liu X, Zhang H. Fe_3O_4@MoS_2@PEI-facilitated enzyme tethering for efficient removal of persistent organic pollutants in water. Chemical Engineering Journal, 2019, 375(1): 121947
26. Xia T T, Liu C Z, Hu J H, Guo C. Improved performance of immobilized laccase on amine-functioned magnetic Fe_3O_4 nanoparticles modified with polyethylenimine. Chemical Engineering Journal, 2016, 295: 201–206
27. Yang X Y, Chen Y F, Yao S, Qian J Q, Guo H, Cai X H. Preparation of immobilized lipase on magnetic nanoparticles dialdehyde starch. Carbohydrate Polymers, 2019, 218: 324–332
28. Qiu X, Wang Y, Xue Y, Li W X, Hu Y. Laccase immobilized on magnetic nanoparticles modified by amino-functionalized ionic liquid via dialdehyde starch for phenolic compounds biodegradation. Chemical Engineering Journal, 2020, 391: 123564
29. Tang R, Du Y, Fan L. Dialdehyde starch-crosslinked chitosan films and their antimicrobial effects. Journal of Polymer Science Part B: Polymer Physics, 2003, 41(9): 993–997
30. Gao J, Zhou J, Zhang X, Shi Q, Han Z, Chen Y. Facile functionalized mesoporous silica using biomimetic method as new matrix for preparation of shape: tabilized phase-change material with improved enthalpy. International Journal of Energy Research, 2019, 43(14): 8649–8659
31. Bradford M M. A rapid and sensitive method for the quantitation of microgram quantities of protein utilizing the principle of protein–dye binding. Analytical Biochemistry, 1976, 72(1-2):

248–254
32. Wahab W A A, Karam E A, Hassan M E, Kansoh A L, Esawy M A, Awad G E A. Optimization of pectinase immobilization on grafted alginate-agar gel beads by 2(4) full factorial CCD and thermodynamic profiling for evaluating of operational covalent immobilization. International Journal of Biological Macromolecules, 2018, 113: 159–170
33. Birhanli E, Noma S A A, Boran F, Ulu A, Yesilada O, Ates B. Design of laccase–metal–organic framework hybrid constructs for biocatalytic removal of textile dyes. Chemosphere, 2022, 292: 133382
34. Gascón V, Márquez-Álvarez C, Blanco R M. Efficient retention of laccase by non-covalent immobilization on amino-functionalized ordered mesoporous silica. Applied Catalysis A: General, 2014, 482: 116–126
35. Xiang X R, Ding S, Suo H B, Xu C, Gao Z, Hu Y. Fabrication of chitosan-mesoporous silica SBA-15 nanocomposites via functional ionic liquid as the bridging agent for PPL immobilization. Carbohydrate Polymers, 2018, 182: 245–253
36. Guo H, Lei B S, Yu J W, Chen Y F, Qian J Q. Immobilization of lipase by dialdehyde cellulose crosslinked magnetic nanoparticles. International Journal of Biological Macromolecules, 2021, 185: 287–296
37. Chen C, Sun W, Lv H Y, Li H, Wang Y B, Wang P. Spacer arm-facilitated tethering of laccase on magnetic polydopamine nanoparticles for efficient biocatalytic water treatment. Chemical Engineering Journal, 2018, 350: 949–959
38. Hu T G, Cheng J H, Zhang B B, Lou W Y, Zong M H. Immobilization of alkaline protease on amino-functionalized magnetic nanoparticles and its efficient use for preparation of oat polypeptides. Industrial & Engineering Chemistry Research, 2015, 54(17): 4689–4698
39. Xie W L, Zang X Z. Lipase immobilized on ionic liquid-functionalized magnetic silica composites as a magnetic biocatalyst for production of trans-free plastic fats. Food Chemistry, 2018, 257: 15–22
40. Hou C, Qi Z G, Zhu H. Preparation of core–shell magnetic polydopamine/alginate biocomposite for candida rugosa lipase immobilization. Colloids and Surfaces B: Biointerfaces, 2015, 128: 544–551
41. Liu R J, Huang W, Pan S, Li Y, Yu L L, He D W. Covalent immobilization and characterization of penicillin G acylase on magnetic Fe_2O_3/Fe_3O_4 heterostructure nanoparticles prepared via a novel solution combustion and gel calcination process. International Journal of Biological Macromolecules, 2020, 162(21): 1587–1596
42. Huang W, Pan S, Li Y, Yu L L, Liu R J. Immobilization and characterization of cellulase on hydroxy and aldehyde functionalized magnetic Fe_2O_3/Fe_3O_4 nanocomposites prepared via a novel rapid combustion process. International Journal of Biological Macromolecules, 2020, 162(21): 845–852
43. Dhiman S, Srivastava B, Singh G, Khatri M, Arya S K. Immobilization of mannanase on sodium alginate-grafted-beta-cyclodextrin: an easy and cost effective approach for the improvement of enzyme properties. International Journal of Biological Macromolecules, 2020, 156: 1347–1358
44. Ahmed S A, Saleh S A A, Abdel-Hameed S A M, Fayad A M. Catalytic, kinetic and thermodynamic properties of free and immobilized caseinase on mica glass-ceramics. Heliyon, 2019, 5(5): 1–12
45. Wehaidy H R, Abdel-Naby M A, El-Hennawi H M, Youssef H F. Nanoporous zeolite-x as a new carrier for laccase immobilization and its application in dyes decolorization. Biocatalysis and Agricultural Biotechnology, 2019, 19: 101135
46. Qiu X, Wang S S, Miao S S, Suo H B, Xu H J, Hu Y. Co-immobilization of laccase and ABTS onto amino-functionalized ionic liquid-modified magnetic chitosan nanoparticles for pollutants removal. Journal of Hazardous Materials, 2021, 401: 123353
47. Wu E H, Li Y X, Huang Q, Yang Z K, Wei A Y, Hu Q. Laccase immobilization on amino-functionalized magnetic metal organic framework for phenolic compound removal. Chemosphere, 2019, 233: 327–335
48. Chao C, Liu J D, Wang J T, Zhang Y W, Zhang B, Zhang Y T, Xiang X, Chen R F. Surface modification of halloysite nanotubes with dopamine for enzyme immobilization. ACS Applied Materials & Interfaces, 2013, 5(21): 10559–10564
49. Mohammadi M, As'habi M A, Salehi P, Yousefi M, Nazari M, Brask J. Immobilization of laccase on epoxy-functionalized silica and its application in biodegradation of phenolic compounds. International Journal of Biological Macromolecules, 2018, 109: 443–447
50. Pang R, Li M Z, Zhang C D. Degradation of phenolic compounds by laccase immobilized on carbon nanomaterials: diffusional limitation investigation. Talanta, 2015, 131: 38–45
51. Ren D J, Jiang S, Fu L J, Wang Z B, Zhang S Q, Zhang X Q, Gong X Y, Chen W S. Laccase immobilized on amino-functionalized magnetic Fe_3O_4–SiO_2 core–shell material for 2,4-dichlorophenol removal. Environmental Technology, 2021, 3: 1–22
52. Chen Z H, Yao J, Ma B, Liu B, Kim J, Li H, Zhu X Z, Zhao C C, Amde M. A robust biocatalyst based on laccase immobilized superparamagnetic Fe_3O_4@SiO_2-NH_2 nanoparticles and its application for degradation of chlorophenols. Chemosphere, 2022, 291(1): 132727
53. Huan W W, Yang Y X, Wu B, Yuan H M, Zhang Y N, Liu X N. Degradation of 2,4-DCP by theimmobilized laccase on the carrier of Fe_3O_4@SiO_2-NH_2. Chinese Journal of Chemistry, 2012, 30(12): 2849–2860
54. Yang J, Hu Y, Jiang L, Zou B, Jia R, Huang H. Enhancing the catalytic properties of porcine pancreatic lipase by immobilization on SBA-15 modified by functionalized ionic liquid. Biochemical Engineering Journal, 2013, 70: 46–54